

Temperature Measurement of Reacting Flowfield by Phase-Shifting Holographic Interferometry

Sheng Mao Tieng* and Wen Zen Lai†

National Cheng Kung University, Tainan, Taiwan 70101, Republic of China

Application of phase-shift holographic interferometry to the temperature measurement of an axisymmetrically premixed flame was experimentally investigated. The test apparatus is an axisymmetric Bunsen burner. Commercial nature hydrocarbon gases were used as the gaseous fuel. A fast Fourier transform for Abel inversion was used to reconstruct the axisymmetric temperature field from the interferometric data. The temperature distribution was compared with thermocouple measurements. The comparison shows that the proposed technique is satisfactory. Errors introduced in the measurement are analyzed and discussed.

I. Introduction

TEMPERATURE scalar distribution is one of the primary quantities that characterizes a given reacting flow, and the techniques for measuring the complex temperature field play a significant role in experimental combustion research. For example, to understand the contribution of heat transfer to flame extinction in a stratified fuel-air mixture, it is necessary to measure the temperature distribution in the flame at the time of extinction. However, such techniques have progressed little, because they have been limited mainly to pointwise measurement. Laser holographic interferometry is a potential technique for remote, nonintrusive, two- or three-dimensional simultaneous measurement.^{1–5} Fisher and Fitzgerald² applied this technique to temperature measurements in a gas-filled incandescent lamp. South and Hayward³ made temperature measurements for an axisymmetric diffusion flame of methane by a single-beam laser holographic interferometry. Reuss⁴ measured the temperature distribution of premixed, lean propane-air flame with this technique. Reuss and Schultz⁵ further used the double-exposure holographic interferometry to determine the instant temperature distribution of a propagating premixed flame in a cylindrical tube.

However, there are several limitations associated with the conventional holographic interferometry technique in its application to temperature measurement of thermal flowfield. For example, the data obtained from the holographic fringe pattern are generally available only at the positions of the intensity minima and maxima of the interferometric fringes. Data at other points are usually obtained only by approximate interpolation,^{6,7} which can lead to considerable errors. Although a scanning microphotometer system can be also used⁴ to obtain more interferometric data, the accuracy and reliability of the results are rigorously restricted by optical noise and the fluctuation of background intensity that are unavoidable in the fringe pattern. Also, for flowfield diagnosis by this technique, a sign ambiguity in fringe order number arises because positive phase and negative phase yield identical fringe patterns. It is the purpose of this work to apply recently developed digital phase shift holographic interferometry⁸ to temperature measurement of reacting flow in order to circumvent effectively the above mentioned limitations of the conventional holographic interferometry.

On the other hand, determination of a temperature field by interferometric fringes relates to the reconstruction of the

refractive index field from the measured projections of interferometric values; that is, the phase data. In the axisymmetric case, Abel inversion is usually used for this reconstruction. However, because the phase data generally are obtained from the conventional holographic interferometry only at a limited number of discrete locations, the Abel inversion scheme is necessarily based on different numerical approximations,⁹ such as the step function method,¹⁰ the linear approximation method,¹¹ the Nestor and Olsen¹² method, and the sampling series method,¹³ which require in most cases a considerably large number of calculations with a lower accuracy. Therefore, in many research fields the search for a faster, more efficient and accurate approach for Abel inversion has become a topic of interest.^{14–17}

Contrary to conventional holographic interferometry, phase shift holographic interferometry has the capability to provide a large amount of phase data. Therefore, the fast Fourier transform was proposed for use in the process of Abel inversion in order to enhance the processing speed and improve the data accuracy. According to our best knowledge, it is the first time that this approach has been applied to the holographic measurement of an axisymmetric flame.

In this work, application of this new technique to temperature measurement of an axisymmetrically premixed flame was experimentally investigated. A modified recording system for the two reference beams, phase-shifting holographic interferometry was set up for this experiment. The reconstructed temperature distributions were compared with thermocouple measurements. The error sources are discussed and the numerical evaluation of the fast Fourier transform, based on Abel inversion, is also conducted.

II. Principles

In the conventional holographic interferometry technique, the image intensity of a holographic interferogram is given by the following equation⁹

$$I(x, y) = I_0(x, y)\{1 + m(x, y)\cos[\Psi(x, y)]\} \quad (1)$$

where $I_0(x, y)$ is the background intensity, $m(x, y)$ is the fringe constant, and $\Psi(x, y)$ is the unknown interferometric phase.

In order to determine the phase value $\Psi(x, y)$ in digital phase-shift interferometry, bias phase ϕ is introduced artificially. This procedure is called phase shifting. Then the image intensity changes as follows:

$$I_i(x, y) = I_0(x, y)\{1 + m(x, y)\cos[\Psi(x, y) + \phi_i]\} \quad (2)$$

For different bias phases ϕ_i , we can obtain different $I_i(x, y)$ of image irradiance distributions. The unknown phase $\Psi(x, y)$

Presented as Paper 91-1388 at the AIAA 26th Thermophysics Conference, Hawaii, June 24–26, 1991. Copyright © 1991 by the American Institute of Aeronautics and Astronautics, Inc. All rights reserved.

*Associate Professor, Institute of Aeronautics and Astronautics, Member AIAA.

†Graduate Student, Institute of Aeronautics and Astronautics.

y) then can be determined from the values of $I_i(x, y)$ and ϕ_i by using the algebraic relationship¹⁸

$$-\Psi(x, y) = \tan^{-1} \frac{\sum_{i=1}^N I_i(x, y) \sin \phi_i}{\sum_{i=1}^N I_i(x, y) \cos \phi_i} \quad (3)$$

where $\phi_i = (i - 1)2\pi/N$ are the stepped bias phases from zero to 2π and N is the step numbers.

From Eq. (3) it is evident that:

1. The total phase distribution $\Psi(x, y)$ can be directly calculated by Eq. (3).
2. The phase-sign ambiguity of the interferometric fringes is eliminated. A negative discontinuity indicates an increase

in fringe number and positive discontinuity a decrease number.

3. $\Psi(x, y)$ is independent of the $m(x, y)$ and $I_0(x, y)$. This means that $\Psi(x, y)$ is not sensitive to some image defects, noise, and the background irradiance or fringe contrast.

Figure 1 shows the earlier arrangement used for pulsed digital, phase-shifting holographic interferometry applied to flow experiments.¹⁸

Determination of an axisymmetric temperature field by interferometric fringes relates to the reconstruction of the refractive index field from measured projections of interferometric values; that is, the phase data $\Psi(x)$ of a ray, which is reconstructed by Abel transform⁹

$$\Psi(x) = \frac{4\pi}{\lambda} \int_x^R \frac{[n(r) - n_0]r \, dr}{[r^2 - x^2]^{1/2}} \quad (4)$$

where $\Psi(x)$ represents the phase data obtained from the phase-shift holographic interferogram; r and x are defined in Fig. 2; $n(r)$ and n_0 denote the refractive index at r and the reference refractive index, respectively. The objective is to determine $n(r)$ from the known phase data $\Psi(x)$.

The inverse of Abel transform is

$$n(r) - n_0 = -\frac{\lambda}{2\pi^2} \int_r^\infty \frac{d\Psi(x)}{dx} (x^2 - r^2)^{-1/2} dx \quad (5)$$

A fast Fourier transform algorithm can be applied to this Abel inversion. The inversion scheme of this method is to perform a Fourier expansion of the data $\Psi(x)$ and calculate the Abel inversion of each spatial frequency component.

To analyze this method, assume $\Psi(x)$ is continuous, symmetric about $x = 0$ and has zero values at and outside the flow boundaries ($\Psi(x) = 0$ for $x \geq R$ or $x \leq -R$). Under these assumptions, $\Psi(x)$ may be written as a cosine expansion

$$\Psi(x) = a_0 + \sum_{m=1}^{+\infty} a_m \cos \frac{m\pi x}{R} \quad (6)$$

$$a_m = \frac{2}{R} \int_0^R \Psi(x) \cos \frac{m\pi x}{R} dx \quad (7)$$

Substituting Eq. (6) into the Abel inversion Eq. (5), we obtain

$$n(r) - n_0 = -\frac{\lambda}{2\pi^2} \int_r^R \frac{d\Psi(x)}{dx} (x^2 - r^2)^{-1/2} dx \quad (8)$$

Let

$$H = \frac{(x^2 - r^2)^{1/2}}{R}, \quad \ell = \frac{r}{R} \quad (9)$$

and Eq. (8) can be written as

$$n(r) - n_0 = \frac{\lambda}{4R} \sum_{m=1}^{\infty} m a_m Q_m(\ell) \quad (10)$$

where

$$Q_m(\ell) = \frac{2}{\pi} \int_0^{(1-\ell^2)^{1/2}} (H^2 + \ell^2)^{1/2} \sin m\pi(H^2 + \ell^2)^{1/2} dH \quad (11)$$

which is defined in interval $[-1, 1]$. Therefore, the Abel inversion of $\Psi(x)$ can be expanded into a sum of the orthogonal basis function $Q_m(\ell)$ with expansion coefficients, which can be simply calculated from the Fourier coefficients of $\Psi(x)$ according to Eq. (7).

If the refraction index distribution $n(r) - n_0$ is calculated from the interferometric phase data using the Abel inversion described above, the fluid density $\rho(r)$ can be obtained through the Gladstone-Dale relation

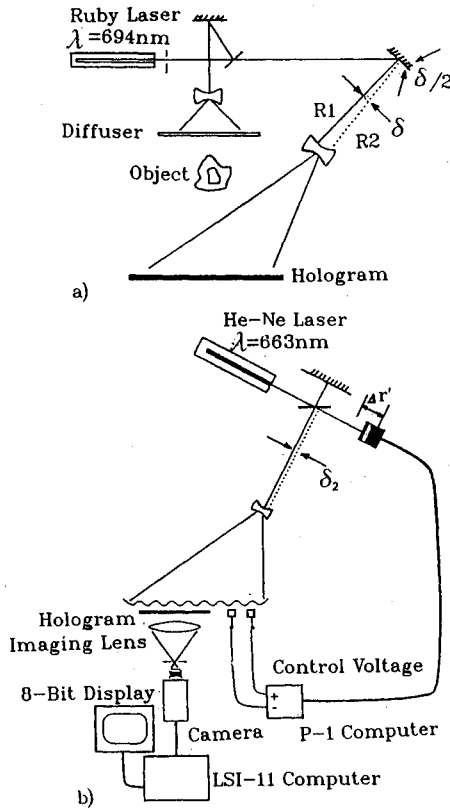


Fig. 1 Conventional optical arrangement for pulsed digital phase shifting holographic interferometry applied to flow experiments¹⁸: a) recording setup; b) reconstruction setup.

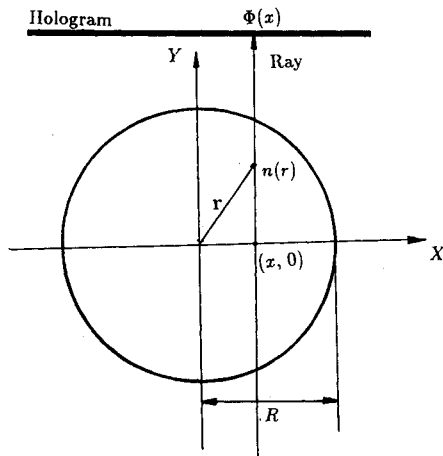


Fig. 2 Schematic diagram of the horizontal cross section of an axisymmetric field.

$$n(r) - 1 = \rho(r) \langle R_G \rangle = \rho(r) \sum_i \beta_i R_{Gi} \quad (12)$$

where β_i and R_{Gi} are the mole fractions and the Gladstone-Dale constants for the species i , respectively.

The Gladstone-Dale constant can be related to the molar refractivity R_{Li}^{19}

$$R_{Gi} \approx 3/2 R_{Li} \quad (13)$$

The molar refractivity R_{Li} is a function of laser wavelength and gas species, and its values for most combustion gases can be found in Ref. 19.

Finally, the temperature distribution is calculated from the density distribution using the perfect gas law as follows:

$$T(r) = T_0 \frac{n_0 - 1}{n(r) - 1} \cdot \frac{\langle R_G \rangle}{R_{G0}} \quad (14)$$

where R_{G0} represents the Gladstone-Dale constant for ambient air. The mole fraction and molar refractivity of the gas mixture are calculated from the reaction equation with given equivalence ratio on the assumption of complete combustion.

According to Ref. 19, the calculated $\langle R_G \rangle_r$ (for reactants of commercial natural hydrocarbon gases including gases of CH_4 , C_2H_4 , C_3H_8 , C_4H_{10} , N_2 , and O_2), $\langle R_G \rangle_p$ (for products including the gases of H_2O , CO_2 , and N_2) and R_{G0} (for ambient air) are 6.6645, 6.891, and 6.2835, respectively, at light wavelength of 6940 Å. $\langle R_G \rangle$ in Eq. (14) is approximately taken as the arithmetical average over $\langle R_G \rangle_r$ and $\langle R_G \rangle_p$

$$\langle R_G \rangle = \frac{\langle R_G \rangle_r + \langle R_G \rangle_p}{2} = 6.777 \quad (15)$$

III. Experiment

A. Optical System

The optical systems used in our experiment are shown schematically in Fig. 3 (for recording), and Fig. 1b (for reconstruction). Unlike the recording system shown as Fig. 1a, which was proposed by Watt and Vest,¹⁸ a modified recording system (see Fig. 3) was set up in our experiment by introducing a slightly misaligned Mach Zehnder interferometer including a Pockels Cell switch for two reference beams, double-exposure recording.

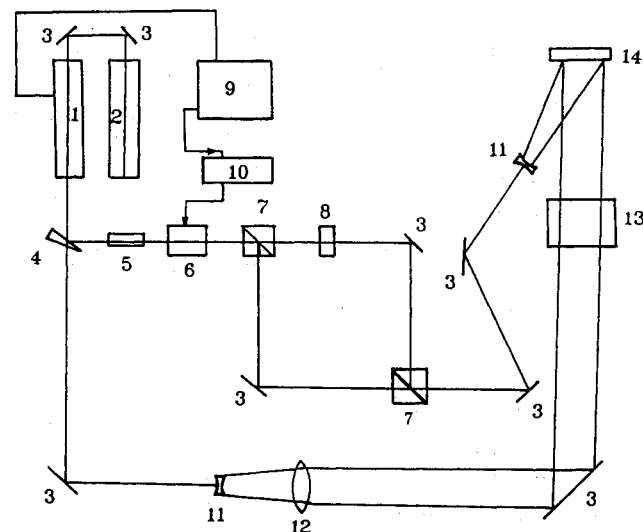


Fig. 3 Improved recording setup: 1) pulsed ruby laser; 2) He - Ne laser; 3) plane mirror; 4) optical wedge; 5) beam expander; 6) Pockels cell; 7) polarized beamsplitter; 8) $\lambda/2$ waveplate; 9) power supply for ruby laser; 10) power supply for Pockels cell; 11) negative lens; 12) positive lens; 13) test section; and 14) hologram plate.

In the double-exposure recording and phase shifting reconstruction processes, two reference/reconstruction beams with a small angular separation are used for reducing the misalignment error due to the complete separation of the recording and reconstruction, and compensating the chromatic error due to the wavelength difference between the recording laser and the reconstruction laser.¹⁸

In recording system (see Fig. 3), a Q-switch pulsed ruby laser (model HLS-2, Lumonics Ltd.) with an output of 1J per pulse and 25-ns pulse duration was used as the light source. The laser beam is collimated by a beam expander and splitted to an object beam and a reference beam by an optical wedge. The reference beam is inducted to a switched Mach-Zehnder interferometer. The purpose of this unit is to switch the linear polarized laser pulses optically, so that the two reference laser pulses used for double exposures transverse different paths in the Mach-Zehnder interferometer. This is done by a Pockels Cell, a polarized beamsplitter, and a $\lambda/2$ wave plate (see Fig. 3). No DC voltage is applied to the Pockels Cell as the first laser pulse comes. Polarization rotation of 90 deg for the second laser pulse occurs when a dc voltage $V_{\lambda/2}$ is applied. So, the two laser pulses with different polarizations transverse different paths by using the polarized beamsplitter. The $\lambda/2$ wave plate is arranged to rotate the polarization of one laser pulses again by 90 deg in order to induce the interference of the two laser pulses with the same polarization. This Mach-Zehnder interferometer is slightly misaligned by turning the plane mirror, so that the two reference beams are tilted with a small angle to form a linear fringe pattern with a space of 1 ~ 2 mm in the hologram.

If the Pockels Cell is switched synchronously to the laser pulses by electrical trigger pulses, this recording system should be available for fast double-pulsed laser holographic interferometry, which is a useful technique for high-speed, unsteady flow diagnostics.

The reconstruction system is the same as the set-up shown in Fig. 1b. A 30-mW He-Ne laser is employed. A slightly misaligned Michelson interferometer provides two reconstruction beams with a small angular separation to form the linear interference fringes. This small angle is adjusted, so that linear fringe pattern on the hologram coincides exactly with the fringe pattern formed by the two reference laser pulses during the recording process. This procedure is performed by means of the Moiré technique. Intersection of the two linear fringe patterns will produce a Moiré pattern and if these two fringe patterns are exactly overlapped, the Moiré pattern disappears.

One plane mirror of the Michelson interferometer is mounted on a piezo translator to which a dc voltage is applied for changing the relative pathlengths of the two reconstruction beams in order to introduce phase shifting. This dc voltage can be adjusted by a dc amplifier controlled by a D/A converter so as to achieve the necessary phase shifting. The Piezoelectric Translator (PZT) nonlinearity is controlled and calibrated by computer.

The phase-shifted interferograms were viewed by a video-camera. The objective lens with a low f -stop number of the videocamera was chosen ($f = 2$) and set close to the hologram plate, so that the linear fringe pattern on the interferogram is outside the image plane. The videocamera and the dc amplifier are connected with a microcomputer.

The camera output is digitized in real time by 8-bit A/D converter with programmable look-up tables (LUT), and stored in a frame buffer. Thus, during a video-cycle of 40 ms, a digitalized image is produced consisting of 512 pixels per line. Every pixel is quantized in 8 bits, that is, in 256 possible gray levels. This digitized image is processed according to an image analysis and phase evaluation software. The computered results are filed on an image storage page. Four image storage pages are available in our image analysis board. Three output D/A converters with LUTs allow monochromatic or chromatic image reproduction on peripherals, such as RGB mon-

itor and thermal color printer (512×512 points on DINA4, 16 colors, and 16 gray levels).

In our test case, three phase-shift steps (0, 120, and 240 deg) were carried out. For every phase-shift step, the micro-computer processes three irradiance values (I_1 , I_2 , and I_3) at each point of the images, which correspond to phase of Ψ , $\Psi + 120$ deg and $\Psi + 240$ deg, respectively. Then the unknown phase distribution can be calculated according to the Eq. (3)

$$\Psi(x, y) = \arctan \frac{\sqrt{3}(I_3 - I_2)}{2I_1 - I_2 - I_3} \quad (16)$$

It should be pointed out that, by using the modified recording system and some techniques in this experiment, such as computer PZT calibration, introducing a slightly misaligned Mach-Zehnder interferometer, low f-stop image lens very close to the hologram, various errors introduced by the phase-shift technique itself should be expected to be suppressed. This is discussed in Sec. IV.

B. Test Apparatus

The application of this phase-shift, holographic interferometry combined with a fast Fourier transform-based Abel inversion is demonstrated by temperature measurement of an axisymmetric premixed flame. In this experiment, the test apparatus was an axisymmetric Bunsen burner with dimensions of 20-mm i.d., 27-mm o.d. and 160-mm height. At the top of the burner a 52 mesh metal screen was set to stabilize the flame. The commercial natural hydrocarbon gases and air are mixed in an air tank and then flow into the burner as gaseous fuel. Information of test flame is described as follows: ratio of mass flow rate, 0.1:1.25 (natural gases: air); inlet velocity, 0.06 m/s; inlet temperature, 350 K; and, inlet Reynolds number, 58. The commercial natural gaseous fuel is composed of methane (54.3%), ethane (16.3%), propane (16.2%), butane, nitrogen (5.8%), and all heavier hydrocarbons (7.4%). The schematic diagram of the burner and the flame structure are shown in Fig. 4.

In order to examine the reliability of the reconstructed results by the proposed technique, the temperature was also measured pointwise by a micro-thermocouple probe.

The thermocouple is made of Pt wire butt-welded with Pt 10% Rh wire, and is mounted on a two-dimensional traversing stage, which allows the thermocouple to be moved horizontally through the flame and vertically along the axial direction.

IV. Results and Discussion

Figures 5a and 5b show two phase-stepped interferograms of the test flame; one corresponds to the original image, and the other to 120 deg phase shifting image. Figure 6 represents

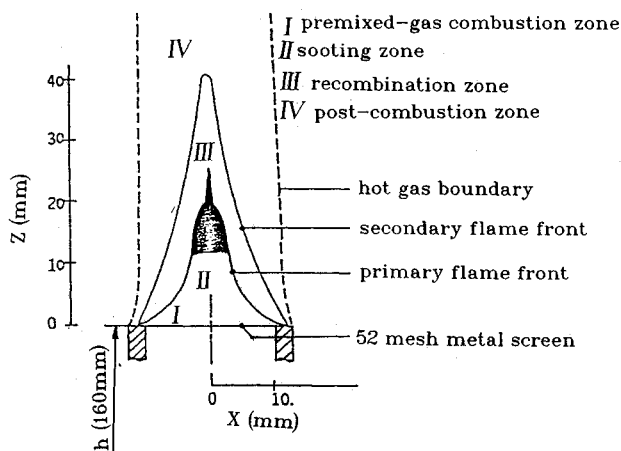


Fig. 4 Schematic diagram of the test Bunsen burner and flame structure.

the image of phase distribution ($\text{mod } 2\pi$) calculated by the phase-shifting procedure. From this phase display we can see clearly the continuous variation of the flow density inside the fringes.

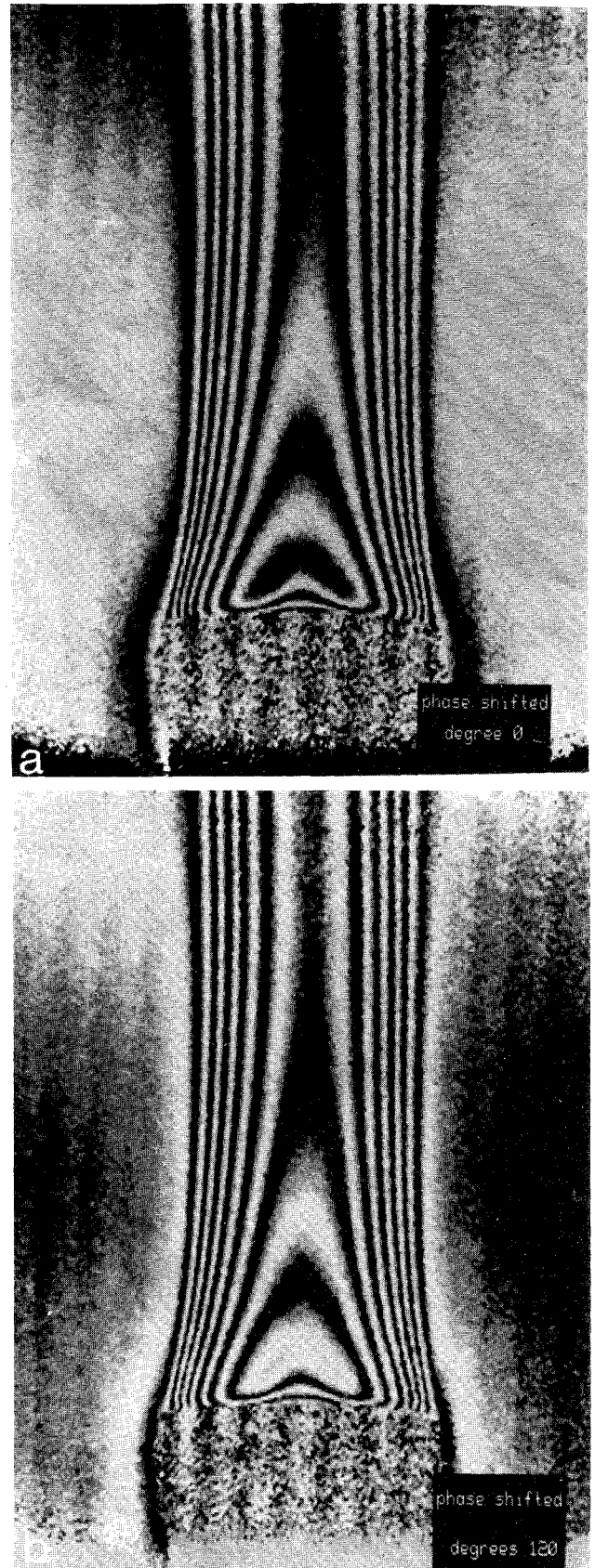


Fig. 5 Holographic interferograms: a) original interferogram of the axisymmetric flame; b) 120-deg phase-shifting interferogram of the flame.

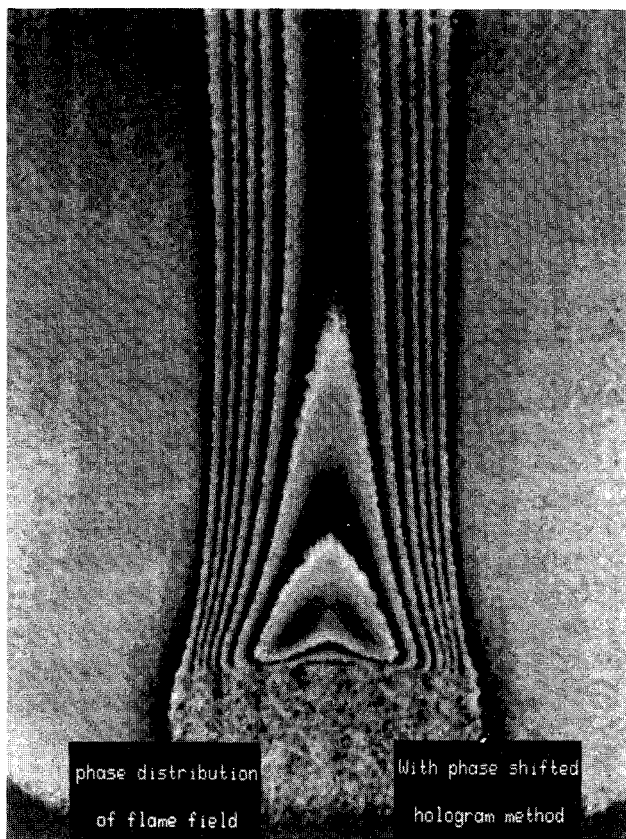


Fig. 6 Image of phase distribution mod 2π calculated by the phase-shifting technique.

Using a sorting program based on the linear discontinuity of the phase distribution, the absolute phase value at each point can be determined. The results are displayed as a monochromatic (gray) scale (normalized to 255 gray levels) and a chromatic scale image by a thermal color printer (see Figs. 7 and 8, respectively).

The refractive index distributions along the lines at AA ($z = 5$ mm), BB ($z = 17$ mm), and CC ($z = 35$ mm) (see Fig. 8 or 9) were reconstructed by the fast Fourier transform-based Abel inversion technique and the temperature distributions along these lines were computed according to the Eq. (14). In this calculation, 20 Fourier expanding terms were used for Abel inversion reconstruction.

The flame temperature distribution was also directly measured by thermocouple. Although the pointwise measurements by thermocouple cannot be considered as an accurate comparison-baseline, both the interferometric data and thermocouple data were plotted in Fig. 9 for comparison. In general, the comparison shows good agreement. So far, for a simultaneous temperature measurement in a whole flame-field, such agreement is satisfactory, although some discrepancies occur. Significant deviations are located in the central and outer regions of the flame. A maximum discrepancy of 110 K occurs at the central axis (see Fig. 9a at $z = 5$ mm). Deviations of 50–100 K can be also found in the large radii ranges from 5 to 8 mm in Fig. 9b and from 8 to 10 mm in Fig. 9c.

The interferometric temperature distribution could be subject to errors introduced by the phase-shift technique and the Abel inversion using Fourier transform. However, the following analysis shows these error sources are not the mechanism causing the deviations mentioned above.

For the phase-shift technique, the errors could be caused by the inaccurate phase steps due to the PZT nonlinearity, spurious interferences due to overlapping cross-reconstructions, hologram misalignment, distortion by image lens, and so forth; also by image intensity noise and phase noise due

to mechanical, thermal, and electrical perturbations. By using the modified recording system and some special technique in this experiment, as described in Sect. III, these errors were effectively suppressed. A test of phase distribution measurement on an undisturbed, quiescent air in ambient temperature was carried out by using the proposed phase-shift technique

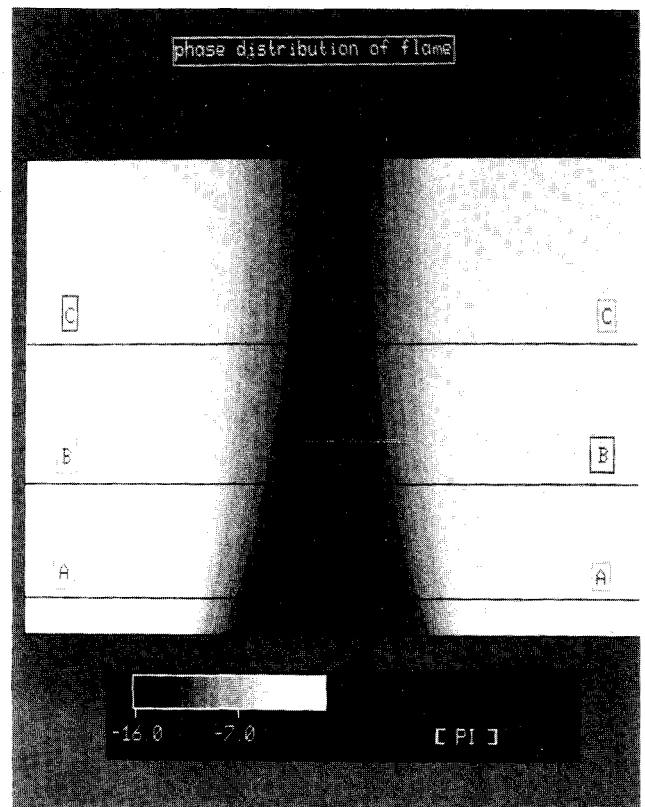


Fig. 7 The absolute phase distribution of the flame displayed as a monochromatic (gray) scale image.

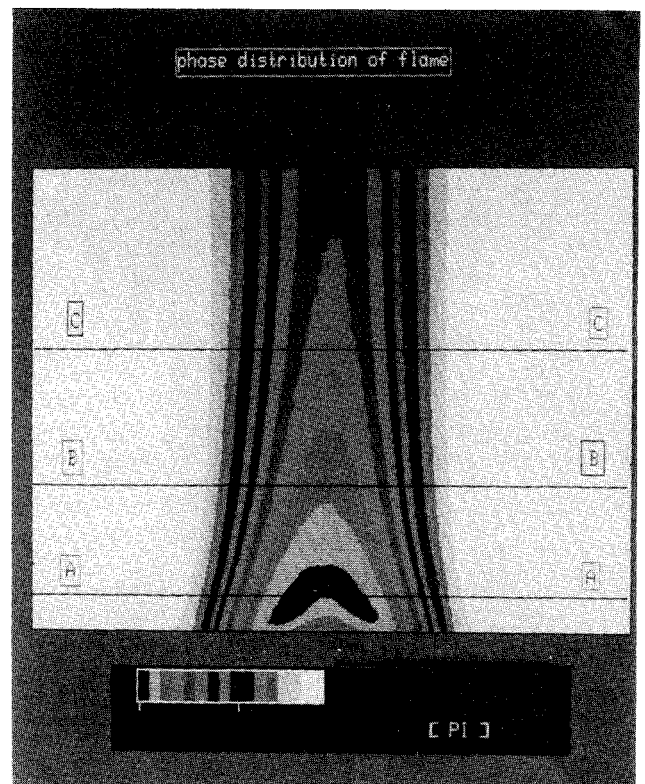


Fig. 8 The absolute phase distribution of the flame displayed as a chromatic scale image.

to evaluate the phase error introduced by this technique. The measured phase data showed that the average phase errors caused by the phase-shift technique were estimated to be about $\delta\psi \approx 1$ deg, which is obviously better than that introduced by conventional holographic interferometry (about $\delta\psi = 15 \sim 20$ deg) as well as by previously reported phase-shift technique (about $\delta\psi = 1.6$ deg).⁸ Corresponding to this phase error, about 1.5 K of temperature errors can be estimated. With such a small phase error, it can be believed that the phase-shift technique does not introduce significant deviations between data measured by the thermocouple and those by the interferometry, as shown in Fig. 9.

The errors resulting from Abel inversion are also very small and can be ignored. Computer simulation was conducted to evaluate this error. A Gaussian model function $e^{-r^2/50}$ as hypothetical refractive index was specified in accordance with the temperature distribution profile of the flame at $z = 35$ mm. The evaluations were taken with different numbers of Fourier transform expanding terms (see Table 1). It is shown that with twenty Fourier expanding terms and 155 grid points (as we did for Abel inversion), the deviation resulting from Abel inversion is only 6.9475×10^{-3} .

The deviations presented in Fig. 9 might be attributed to three major error sources in the temperature determination. They are 1) effect of chemical composition distribution in the flame on the accuracy of the interferometric data; 2) bending of the laser beam traversing the flame; and 3) the random oscillations of the flame make the accurate pointwise measurements very difficult due to the limited spatial and temporary resolutions of the thermoprobe.

The temperature distribution reconstructed by interferometric measurement is determined by Eq. (14). From this equation, it is clearly seen that the composition distribution in reacting flows is required for the reconstruction of interferometric temperatures. Often in the past the composition distribution was either neglected^{4,5} or assumed by a simple relationship,³ owing to lack of the information of composition distribution, as is the case in the present study. Actually, for a reacting flow, Gladstone-Dale constant depends upon different chemical species. But in the present work, because the variation of composition throughout the flame is neglected, the Gladstone-Dale constant was approximately taken as the arithmetical average over $\langle R_G \rangle$, and $\langle R_G \rangle_p$ (see Eq. (15)). This approximation and assumption will introduce considerable errors for the case of fuel-rich premixed flame, as indicated in the recent investigation about the effect of composition change on temperature measurement in premixed flame by holographic interferometry.²⁰ The test flame in the present measurement belongs to fuel-rich one; therefore, it should be reasonable to consider the errors introduced by composition changes in the flame as one of the major errors contributed to the deviations in Fig. 9, especially in the lower region of the flame. As revealed in Ref. 20, the pyrolysis of the reactants occurs immediately once the premixed fuel is injected into the flame, and various hydrocarbons and intermediate species can be found in the lower portion of the flame (especially in the premixed-gas combustion zone), where variation of composition distribution along the radius is large. It has been shown,²⁰ that chemical compositions change greatest in the central portion. Due to this, the Gladstone-Dale constant $\langle R_G \rangle$ as well as the molar refractivity R_L would change significantly with locations. As pointed in Ref. 20, the greatest deviation of molar refractivity R_L between at the axis and at the hot gas boundary (see Fig. 4) is as large as 16% for the case of fuel-rich flame. Therefore, if $\langle R_G \rangle$ is taken as a constant value as we did (Eq. 15), significant errors would be introduced. In particular, the centerline temperature is very sensitive to the change in $\langle R_G \rangle$,⁴ hence maximum deviations (about $\Delta T = 110$ K) appear just at the center axis. However, as the section height of the flame increases, the composition change becomes gradually less significant and this leads to a smaller deviation in central region of the flame, as shown in Figs. 9b and 9c.

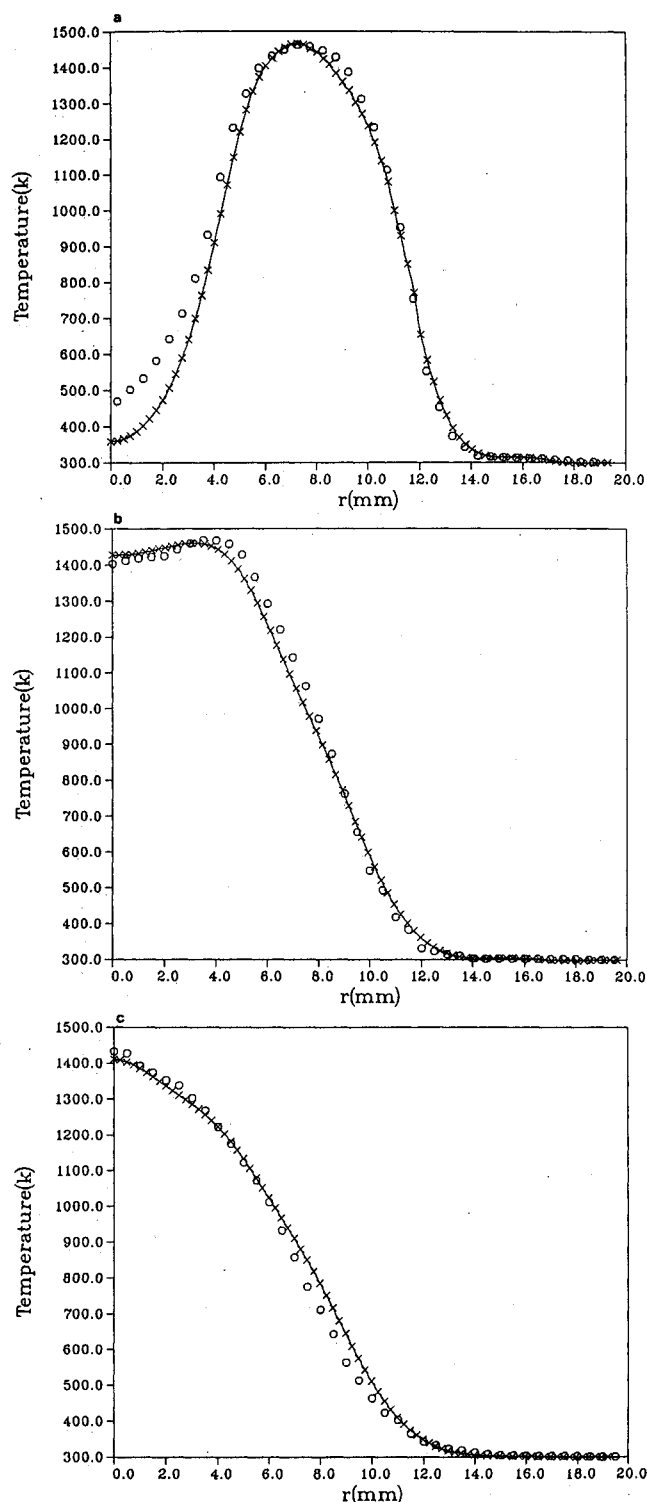


Fig. 9 Temperature distributions along the lines: a) AA at $Z = 5$ mm, b) BB at $Z = 17$ mm, c) CC at $Z = 35$ mm (o, thermocouple-measured values; \times , holographic results).

Table 1 Evaluations for different numbers of Fourier expanding terms

Number of expanding terms	rms deviation
10	6.9621×10^{-3}
15	6.9483×10^{-3}
20	6.9475×10^{-4}
25	6.9427×10^{-3}
30	6.9421×10^{-3}
35	6.9398×10^{-3}
40	6.9393×10^{-3}

Furthermore, due to density gradients, bending of the initially parallel laser beam by the reacting flow can occur. Therefore, the assumption of no refraction required for the Abel inversion may be violated for the flow with strong density gradients. The present investigated flame is of high temperature gradient, substantial ray bending exists and its effect on the accuracy of the interferometric data are not ignored.²¹ Due to the conical shape of the test flame, the traversing path of the beams through the flame increases as the section height decreases. Hence a larger deviation should be expected in the center portion of lower test sections.

Other considerable errors may be caused by pointwise measurements of thermocouple. Random oscillations of the flame make accurate measurement very difficult. Especially, near the hot gas boundary (see Fig. 4), the oscillation gets serious and, at the same time, the temperature gradient is very sharp in this region, thus, errors of thermocouple measurement are expected to be considerably large. Perhaps this is the major reason significant deviations appear in the large radii ranges, as shown in Figs. 9b and 9c. The temperature distribution could be also affected by asymmetry of the flame. However, this was eliminated by taking great care to produce a radially symmetric flame.

Radiation loss correction for thermocouple measurements were not made in this work because the velocity distribution of the reacting flow was not available. If a proper radiation correction were made, the data measured by the thermocouple in high temperature region (>1000 K) might be closer to the interferometric temperatures.

It should be pointed out that the errors introduced by fringe numbering, which usually is determined by interpolation method in conventional holographic interferometry, do not appear in the proposed technique, because accurate phase distribution of the whole interferogram can be determined directly, without fringe counting process. Particularly in the lower portion of the flame where the fringes become broad and indistinct, considerable fringe counting errors will be introduced by interpolation method. Reuss⁴ estimated an interferometric temperature error of 6% at the centerline of the flame due to this fringe counting error.

V. Conclusion

Phase-shift, holographic interferometry combined with Abel inversion using the fast Fourier transform has been successfully applied to temperature measurement of an axisymmetric premixed flame.

As has been shown, the proposed technique improves the accuracy of the interferometric measurement and circumvents the limitation of interpolation for fringe numbering detrimental to the conventional holographic interferometry, especially in the lower portion of the flame where the fringes are mostly broad and indistinct.

As revealed in the Results and Discussion section, the major errors affecting the accuracy of temperature measurement by phase-shift, interferometric technique are not subject to the technique itself, but to the composition change in the flame and to the beam bending traversing the flame. Although, in the case of fuel-rich flame, these errors might be significant, from the viewpoints of simultaneous temperature measurement for a whole flamefield and of accurate determining phase distribution, this technique would provide a potential perspective of temperature measurement in a reacting flow-field, if the major error sources mentioned above were corrected appropriately. Quantitative analysis and correction for these errors in interferometric measurements will be investigated in the near future.

Furthermore, the recording system proposed in this experiment will be available for fast, double-pulsed, phase-shifting holographic interferometry presenting potential application in the high-speed, unsteady flow diagnostics.

Acknowledgments

The authors gratefully acknowledge the financial support of this project by the National Science Council of the Republic of China under Contract NSC 80-0401-E006-32. The authors also thank K. C. Chang for his frequent discussions, which stimulated this investigation.

References

- ¹Trolinger, J. D., "Holographic Interferometry as a Diagnostic Tool for Reacting Flows," *Combustion Science and Technology*, Vol. 13, No. 3, 1976, pp. 229–244.
- ²Fisher, E., and Fitzgerald, J., "Heat and Mass Transport in Cylindrical Gas-filled Incandescent Lamp," *Journal of Applied Physics*, Vol. 45, No. 7, 1974, pp. 2895–2902.
- ³South, R., and Hayward, B. M., "Temperature Measurements in Conical Flames by Laser Interferometry," *Combustion Science and Technology*, Vol. 12, No. 2, 1976, pp. 183–195.
- ⁴Reuss, D. L., "Temperature Measurements in a Radially Symmetric Flame Using Holographic Interferometry," *Combustion and Flame*, Vol. 49, No. 2, 1983, pp. 207–219.
- ⁵Reuss, D. L., and Schultz, P. H., "Interferometric Temperature Measurements of a Flame in a Cylindrical Tube Using Holography," *Applied Optics*, Vol. 26, No. 9, 1987, pp. 1161–1167.
- ⁶Huang, J. M., Chang, K. C., and Tieng, S. M., "Temperature Measurements in Heated Air Jet-like Flows by Laser Holographic Interferometry," *Proceedings of the Fifth International Symposium on Application of Laser Techniques to Fluid Mechanics and Workshop on the Use of Computers in Flow Measurements*, Lisbon, Portugal, July 9–12, 1990.
- ⁷Tieng, S. M., and Chen, H. T., "Holographic Tomography by SART and its Application to Reconstruction of 3D Temperature Distribution," *Wärme-und Stoffübertragung*, Vol. 26, No. 1, 1990, pp. 49–56.
- ⁸Dändliker, R., and Thalmann, R., "Heterodyne and Quasi-heterodyne Holographic Interferometry," *Optical Engineering*, Vol. 24, 1985, p. 824.
- ⁹Vest, C. M., *Holographic Interferometry*, Wiley, New York, 1979.
- ¹⁰Landenburg, R. W., Lewis, W., Phease, W. N., and Taylor, H. S., "Physical Measurements in Gas Dynamics and Combustion," *Proceedings of the High Speed Aerodynamics and Jet Propulsion*, Oxford Univ. Press, Oxford, England, UK, 1955.
- ¹¹Bockasten, K., "Transformation of Observed Radiances into Radial Distribution of the Emission of a Plasma," *Journal of the Optical Society of America*, Vol. 51, 1961, p. 943.
- ¹²Nestor, O. H., and Olsen, N. H., "Numerical Method for Reducing Line and Surface Probe Data," *SIAM Review*, 1960, p. 200.
- ¹³Barakat, R., "Solution of an Abel Integral Equation for Band-Limited Functions by Means of Sampling Theorems," *Journal of Mathematical Physics*, Vol. 43, 1964, pp. 325–331.
- ¹⁴Schardin, H., "Die Schlierenverfahren und ihre Anwendungen," *Ergebnisse der Exakten Naturwissenschaften*, Springer-Verlag, Berlin, 1942, pp. 303–439.
- ¹⁵Ladenburg, R., Winckler, J., and Van Voorhis, C. C., "Interferometric Study of Faster than Sound Phenomena, Part I," *Physical Review*, Vol. 73, 1948, pp. 1359–1377.
- ¹⁶Pikalov, V. V., and Preobrazhenskii, N. G., "Abel Transformation in the Interferometer Holography of a Point Explosion," *Fizika Goreniya i Vzryva [Combustion, Explosion, and Shock Waves]*, Vol. 10, 1975, p. 827.
- ¹⁷Fleurier, C., and Chapelle, J., "Inversion of Abel's Integral Equation: Application to Plasma Spectroscopy," *Computer Physics Communications*, Vol. 7, 1974, p. 200.
- ¹⁸Watt, D. W., and Vest, C. M., "Digital Interferometry for Flow Visualization," *Experiments in Fluids*, Vol. 5, 1987, p. 403.
- ¹⁹Gardiner, W. C., Hidaka, Y., and Tanzawa, T., "Refractivity of Combustion Gases," *Combustion and Flame*, Vol. 40, 1981, pp. 213–219.
- ²⁰Chen, C. C., Chang, K. C., and Tieng, S. M., "Effect of Composition Change on Temperature Measurement in Premixed Flame by Holographic Interferometry," *Optical Engineering*, Vol. 31, 1992, pp. 353–362.
- ²¹Montgomery, C. P., and Reuss, D. L., "Effects of Refraction on Axisymmetric Flame Temperature Measured by Holographic Interferometry," *Applied Optics*, Vol. 21, No. 8, 1982, pp. 1373–1380.